SHEAR-WAVE VELOCITY PROFILES ACROSS THE FERRARA ARC: A CONTRIBUTION FOR ASSESSING THE RECENT ACTIVITY OF BLIND TECTONIC STRUCTURES

N. Abu-Zeid[1], S. Bignardi[1], R. Caputo[1,2], A. Mantovani[1], G. Tarabusi[1,3], G. Santarato[1]
[1] *Department of Physics and Earth Sciences, University of Ferrara, Italy*
[2] *Research & Teaching Centre for Earthquake Geology, Tyrnavos, Greece*
[3] *Istituto Nazionale di Geofisica e Vulcanologia, Sezione Roma 1, Roma, Italy*

Introduction. In the late May 2012, a noticeable seismic sequence affected a wide area of the eastern sector of the Po Plain, causing 27 casualties, thousands of injuries, severe damages to historical centers and industrial areas, and extensive liquefaction phenomena along abandoned river channels (Caputo and Papathanassiou, 2012; Galli *et al*., 2012; GdL Liquefazione RER, 2012; Emergeo Woking Group, 2013; Papathanassiou *et al*., 2012).

The sequence has been characterized by two main shocks, with M_L ranging from 5.9 and 5.8, respectively. The first occurred on May 20 at 02:03 UTC, with epicenter between Finale Emilia and San Felice sul Panaro (44°51'50"N, 11°14'31"E, h = 6.3 km), while the second occurred on May 29 at 07:00 UTC, 15 km SW of the first shock, near Mirandola (Massa *et al*., 2012).

The causative faults of this seismic sequence are two segments of the Ferrara Arc thrust system, which is one of the three major arcs of blind, north-verging thrusts and folds that represent the Apennines front. The Ferrara Arc, with a total length of more than 100 km, is characterized by several second order structures showing a complex internal geometry and, in particular, the activated structures have a left-stepping largely overlapping geometry (Pieri and Groppi, 1981; Bigi *et al*., 1982; Boccaletti *et al*., 2004; Bonini *et al*., 2014). Both these seismogenic sources were associated with blind, mainly dip-slip reverse, faulting (*e.g*. Scognamiglio *et al*., 2012; Pondrelli *et al*., 2012), while the uppermost tip segment of the sliding planes has been estimated to reach a minimum depth of 3-4 km (Bignami *et al*., 2012).

One of the coseismic effects due to the reactivation of reverse blind faults, as in the case of the Po Plain, is the bending of the topographic surface and the consequent uplift of the broader epicentral area. In fact, as a consequence of the fault geometry and kinematics, the rock volume above the co-seismic rupture tip is characterised by a typical fault-propagation folding process (Okada, 1985; Bignami *et al*., 2012; Salvi *et al*., 2012). Depending on the seismotectonic parameters of the underlying seismogenic source, the uplifted area has an elliptical shape that is characterized, in correspondence of the epicentral area, by a maximum vertical displacement of some tens of centimeters. The application of satellite interferometry (DinSAR technique) to the Emilia seismic sequence clearly show that the main shocks of the 20th and 29th of May produced two uplifted areas, characterized by a maximum vertical displacement of 25 cm, partly overlapping and with a cumulative length of about 50 km in E-W direction (Bignami *et al*., 2012; Salvi *et al*., 2012).

The recurrence of similar 'areal morphogenic earthquakes' (Caputo, 2005) and the competition with the high subsidence and depositional rates that characterize the Po Plain, have progressively modified the geomorphology and stratigraphy of the region. In this conditions, the hydrographic network has proven to be particularly sensitive to vertical deformations, so even small altimetric and gradient changes could induce river avulsions and diversions, highlighted by the presence of several drainage anomalies (Burrato *et al*., 2003, 2012). Consequently, the alluvial plain is actually crossed by numerous abandoned river channels, some of which are still well preserved. Obviously, the presence of active tectonic structures responsible for the local uplifts and even for the complex interactions with the hydrographic network has influenced not only the distribution of the sediments on the surface, but also in the subsoil (down to some tens of metres) producing important stratigraphic variations and therefore also changes in the geophysical properties of the materials.

Determining the space distribution of the tectonically induced uplift rate together with the location of active faults is therefore of the utmost concern not only for reconstructing the

tectonic evolution of the region in the past, but also to help understanding where active faults are located, and which is their seismogenic potential. Scenarios of concentration of energy of future events can thus be simulated for mitigating the seismic hazard especially in the more prone areas.

Many direct and indirect data were collected in the Po Plain for hydrocarbon explorations during the past decades, reaching investigation depths often comparable with the foci of the recent earthquakes. Unfortunately, these data are often classified and thus they are hardly available for researchers. However, even when available, for example seismic reflection profiles and gravimetry, the information have insufficient resolution in order to document the most recent activity of the tectonic structures. Indeed, evidences of such activity should be searched for at shallower depths, say within the first few hundreds meters, and this represents the main target of the present reserch.

With this premise and in order to contribute to this task, we planned a geophysical survey across some major tectonic structures affecting the subsoil of the eastern Po Plain. Our investigation is based on several passive seismic measurements carried out along the profiles with a mean distance of 1 km; in particular, we applied the ESAC (Aki, 1957, 1964; Asten and Henstridge, 1984; Ohori *et al*., 2002) and Re.Mi. methods (Louie, 2001; Stephenson et al., 2005), which could provide information in the first 100-150 m. Accordingly, each measurement gives the vertical distribution of the shear waves velocity, *i.e*. 1D models, down to a depth of ca. 150 m. All vertical models have been thus interpolated to generate a pseudo-2D section.

Both profiles are ca. 27 km-long and are oriented SSW-NNE, *i.e*. almost perpendicular to the regional trend of the buried tectonic structures belonging to the central sector of the Ferrara Arc. The western profile runs between Cento and Bondeno, while the eastern one between Traghetto and Formignana (Fig. 1).

In this paper, we describe and comment the profile west of Ferrara, while measurements for the eastern profile are still in progress.

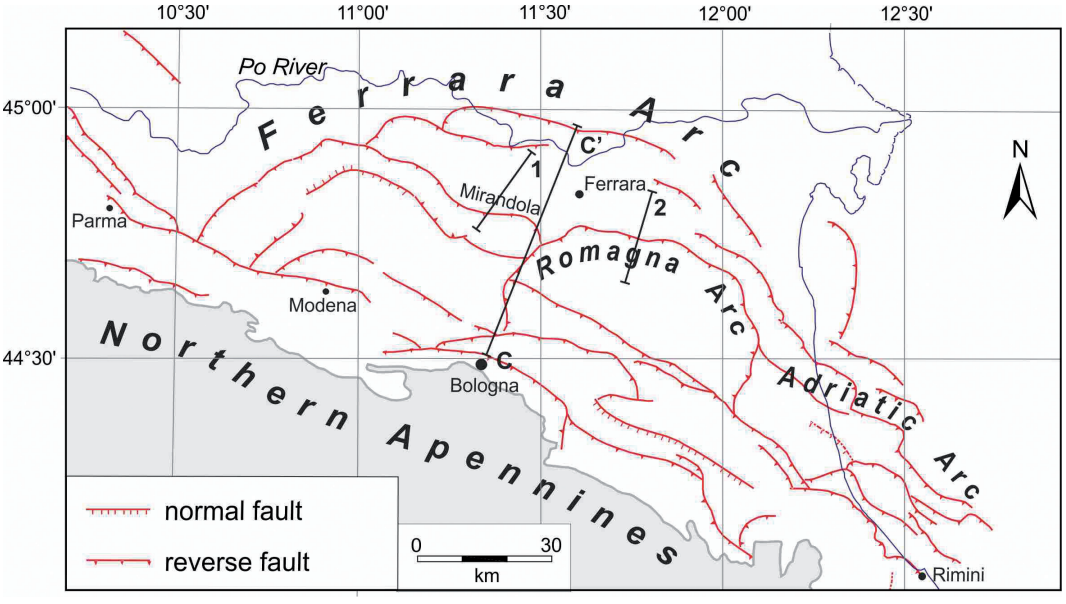

Fig. 1 – Simplified structural map of the eastern sector of the Po Plain showing the major Ferrara Arc and the two minor Adriatic and Romagna arcs. The traces of the measurement profiles (1 and 2) and of a geological section represented in Fig. 3 (C-C') are also shown .

Data acquisition along profile 1. The performed measurements were based on passive seismic techniques, both exploiting the ambient seismic noise: the ESAC and Re.Mi. methods. Both techniques are able to acquire the vertical sequence of shear waves velocity. Along this profile we performed 20 measurements, in particular, 13 acquisitions according to the ESAC procedure and 7 with the Re.Mi. one. In Tab. 1 are reported both kilometric and geographic coordinates of all investigated sites.

The Re.Mi. (*Refraction Microtremors*) method is based on a linear layout of vertical geophones commonly used in seismic refraction surveys. The data analysis is performed via Fourier transform, after a preliminary 'slant stack' operation, and followed by 1D inversion of the fundamental phase. A conceptual limit of this method is due to the fact that only the waves propagating parallel to the geophones layout are properly analysed, while for all other directions the inversion procedure tends to overestimate the shear velocity.

The ESAC (*Extended Spatial AutoCorrelation*) method is characterised by a 2D layout of the geophones located along T- or L-shape profiles. This assures a better coverage of the seismic waves record and avoids the above mentioned directionality problem of the Re.Mi. technique. Inversion of ESAC data is performed in the distance domain for each frequency. The use of the ESAC method is crucial for obtaining information on the velocity distribution at greater depths with respect to Re.Mi. results, while the latter technique is more easily applied in the field for sites with reduced accessibility.

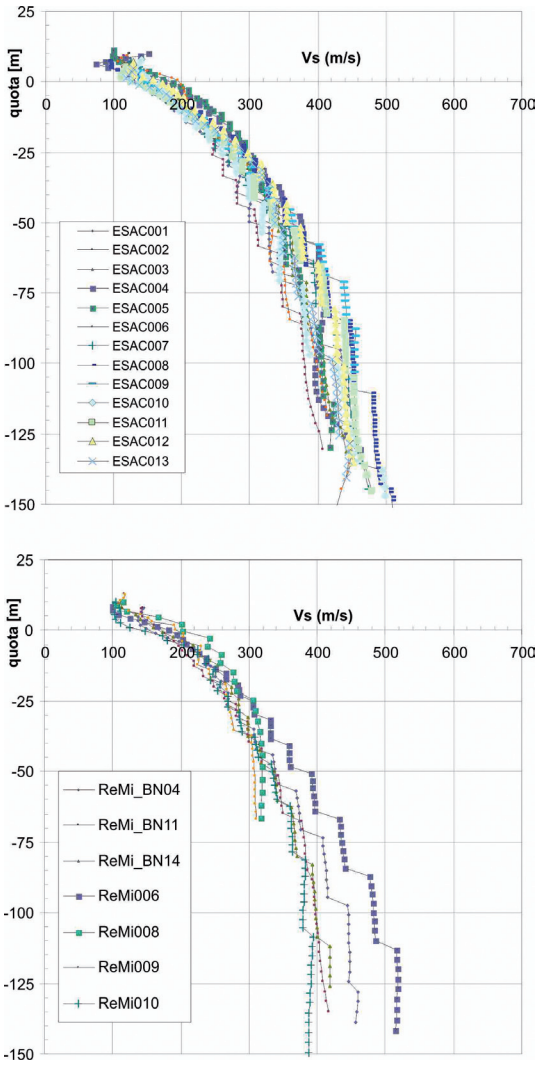

Fig. 2 – The 1D shear-waves velocity profiles obtained using the ESAC (top) and Re.Mi. (bottom) techniques. Site coordinates are reported in Tab. 1.

In each site a layout of 24 3-component geophones (velocimeters), spaced 8 m, was developed and the vertical (vertical Rayleigh component) and one horizontal (Love) components of the particles velocity were acquired using a commercial seismograph, characterized by a 24 bits dynamics.

Inversion of the data was based on a 1D scheme, *i.e.* variation of geophysical parameters only along the vertical axis, using a commercial software (SeisOpt^{tm}, http://www.optimsoftware.com/index.php/seisopt-remi-by-optim-software), and inverting simultaneously Rayleigh and Love velocity *versus* frequency dispersion spectra. Smooth inversion option was selected, based on the Simulated Annealing (SA) algorithm. The relatively long spacing between geophones produced aliasing, but this noise disturbed spectra at frequencies higher than 10-15 Hz, corresponding to the shallowest depths (no more than 10 m), is irrelevant to our analyses.

In Fig. 2, the 1D shear wave velocity profiles obtained by inversion of the fundamental mode dispersion curves of

Tab. 1 - Coordinates of the investigated sites.

site	label	latitude (UTM32N, km)	longitude (UTM32N, km)	latitude (°N)	longitude (°E)
1	Re.Mi._9_R	4955321.342	680148.539	44°43′36.65″	11°16′25.94″
2	ESAC006	4957368.578	681854.073	44°44′50.05″	11°18′09.39″
3	Re.Mi._8_R/L	4959077.820	682045.420	44°45′36.57″	11°17′56.93″
4	ESAC005	4959281.085	683264.939	44°45′45.21″	11°18′55.79″
5	ESAC004	4960660.598	684315.250	44°46′29.00″	11°19′45.62″
6	ESAC003	4961671.719	684777.700	44°47′1.74″	11°20′7.84″
7	Re.Mi._10_R	4962853.122	685783.316	44°47′35.36″	11°20′51.77″
8	ESAC002	4963654.769	687042.923	44°48′3.65″	11°21′53.28″
9	ESAC001	4965371.322	686964.542	44°48′59.74″	11°21′51.88″
10	ESAC010	4966249.194	687756.194	44°49′27.19″	11°22′29.19″
11	Re.Mi._6_R	4967058.276	687402.990	44°49′50.00″	11°22′11.00″
12	ESAC007	4967338.695	688579.199	44°50′1.53″	11°23′7.48″
13	BN_14_R/L	4967883.042	688148.009	44°50′16.00′′	11°22′46.00′′
14	ESAC008	4969384.450	690044.932	44°51′5.80″	11°24′18.89″
15	ESAC011	4971312.633	691557.693	44°52′7.36″	11°25′28.74″
16	BN_04	4972431.908	691392.196	44°52′40.18″	11°25′19.81″
17	ESAC012	4972707.823	692788.281	44°52′50.81″	11°26′27.14″
18	ESAC009	4974040.307	694034.546	44°53′32.68″	11°27′25.94″
19	BN_11_R/L	4974705.786	694270.004	44°53′51.00′′	11°27′34.00″
20	ESAC013	4975796.051	694379.424	44°54′29.48″	11°27′43.13″

Rayleigh waves are represented, for all the sites but separately for the two techniques. Most ESAC profiles show a sharp velocity decrease in the first few meters while velocity progressively increases with depth (Fig. 2, top). Due to the slightly different approach for data inversion, the specific behavior at shallow depth is not observed in the Re.Mi. velocity profiles (Fig. 2, bottom).

Pseudo-2D section. The trace of the profile runs in a SSW-NNE direction from near Cento to the east of Bondeno. The investigated sites laying out of the profile trace, because of topographic or access difficulties, have been perpendicularly projected and their distance from the trace ranges between 60 and 900 m. Although 1D profiles have been locally reconstructed at greater depths, the interpretation of the section has been attempted to a depth of 150 m b.s.l. (considering that the altitude of the investigated sites ranges between 7 and 15 m a.s.l.).

In order to obtain the pseudo-2D velocity section, all 1D projected velocity profiles have been interpolated with different techniques all showing some major features. Due to the similarity of the interpolations, in Fig. 3 only the interpolation obtained by applying the local polynomial method is illustrated and discussed.

If we reasonably assume that the overall pattern of the shear wave velocity is determined by lithological variations, both lateral and vertical ones, especially in terms of different sedimentation rate (*i.e.* different ages at comparable depths), the pseudo-2D section represented in Fig. 3 allows to infer the occurrence of buried anticlinal structures in correspondence with the higher velocity gradients associated with a (more) 'condensed' stratigraphy. Conversely, where velocity gradients are lower, the thickness of the coeval sedimentary units is greater (*i.e.* synclinal structures).

If we compare our results with available geological profiles crossing the same investigated area (Fig. 1), it is possible to observe a good agreement with the occurrence of some major

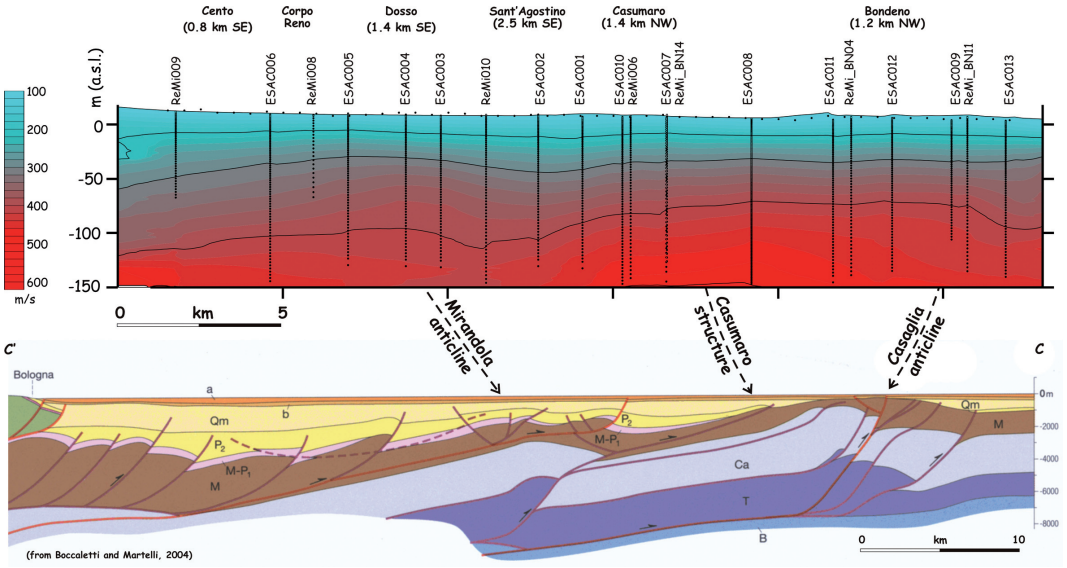

Fig. 3 – The pseudo-2D section (top) showing the shear-waves velocity distribution in the shallow subsoil (first ca. 150 m) as obtained by interpolation of several 1D ESAC and Re.Mi. profiles. Bottom: part of the geological section C-C' from Boccaletti and Martelli (2004) running parallel to the section, ca. 7 km SE (see Fig. 1 for location).

tectonic structures that characterize the subsoil of the region and mainly associated with the recent activity (Late Quaternary) of the Ferrara Arc. In particular, it is possible to correlate the local high velocity gradient observed in the northern part of our profile to the Casaglia anticline, while the southern one likely corresponds to a deeper periclinal setting of the easternmost sector of the Mirandola structure (Fig. 1). The effects on the shallow velocity distribution caused by a secondary structure (here referred to the Casumaro structure) merge with those of the Casaglia anticline thus generating an apparently larger scale unique dome. By increasing the density of 1D velocity profiles along the investigated transect will likely improve the resolution of the pseudo-2D section thus allowing to distinguish the two structures.

Conclusions and future work. The reconstructed velocity profile documents the possibility to detect the recent tectonic activity of buried structures underlying the alluvial Po Plain by means of low-cost geophysical surveys. Indeed the applied techniques does not need expensive equipment nor large teams. The passive seismic techniques allowed to measure in relatively short time numerous 1D velocity profiles down to a depth of 100-150 m (depending on the layout of the geophones). Accordingly, it is possible to carry out a sufficient number of such measurements to confidently interpolate a pseudo-2D section several kilometers-long therefore emphasizing the possible occurrence of lateral shear wave velocity variations corresponding to stratigraphic ones. The comparison with available seismic profiles for hydrocarbon explorations and particularly with the location of the major tectonic structures well documented at greater depths and affecting older rocks suggests that the shallow stratigraphic variations documented in this research are directly associated with a recent activity of the buried folds.

This new methodological approach is being applied for investigating the shallow subsoil across similar structures east of Ferrara (profile 2 in Fig. 1). The data acquisition for this second profile are in progress and will be combined with a microgravimetric 3D survey specifically planned to include the profile.

Aknowledgements. This study has benefited from funding provided by the Italian Presidenza del Consiglio dei Ministri - Dipartimento di Protezione Civile (DPC). This paper does not necessarily represent DPC official opinion and policies. Partly was also supported by the Province of Ferrara, DPC Unit and municipalities of Argenta, Ferrara, Bondeno and Comacchio.

References

Aki K. (1957): Space and time spectra of stationary stochastic waves, with special reference to microtremors, *Bull. Earthquake Res. Inst.*. **35**, 415-456.

Aki K. (1964): A note on the use of microseisms in determining the shallow structures of the earth's crust. *Geophysics*. **29**, 665-666.

Asten M.W. and Henstridge J.D. (1984): Array estimators and the use of microseisms for reconnaissance of sedimentary basins. *Geophysics*, **49**, 1828-1837.

Bigi G., Bonardini G., Catalano R., Cosentino D., Lentini F., Parlotto M. Sartori R., Scandone P. and Turco E. (1992): *Structural model of Italy, 1:500,000*. Consiglio Nazionale delle Ricerche, Roma.

Bignami C., Burrato P., Cannelli V., Chini M., Falcucci E., Ferretti A., Gori S., Kyriakopoulos C., Melini D., Moro M., Novali F., Saroli M., Stramondo S., Valensise G. and Vannoli P. (2012): Coseismic deformation pattern of the Emilia 2012 seismic sequence imaged by Radarsat-1 interferometry. *Annals of Geophys.*, **55**(4), 788-795, doi: 10.4401/ag-6157.

Boccaletti M., Bonini M., Corti G., Gasperini P., Martelli L., Piccardi L., Tanini C. and Vannucci G. (2004): *Seismotectonic Map of the Emilia-Romagna Region, 1:250000*. Regione Emilia-Romagna – CNR.

Bonini L., Toscani G. and Seno S. (2014): Three- dimensional segmentation and different rupture behavior during the 2012 Emilia seismic sequence (Northern Italy). *Tectonophys.*, **630**, 33-42, doi: 10.1016/j.tecto.2014.05.006.

Burrato P., Ciucci F. and Valensise G. (2003): An inventory of river anomalies in the Po Plain, northern Italy: evidence for active blind thrust faulting. *Annals of Geophys.*, **46**(5), 865-882.

Burrato P., Vannoli P., Fracassi U., Basili R. and Valensise G. (2012): Is blind faulting truly invisible? Tectonic-controlled drainage evolution in the epicentral area of the May 2012, Emilia-Romagna earthquake sequence (northern Italy). *Annals of Geophys.*, **55**(4), 525-531, doi: 10.4401/ag-6182.

Caputo R. (2005): Ground effects of large morphogenic earthquakes. J. Geodyn., 40(2-3), 113-118.

Caputo R. and Papathanasiou G. (2012): Ground failure and liquefaction phenomena triggered by the 20 May, 2012 Emilia-Romagna (Northern Italy) earthquake: case study of Sant'Agostino - San Carlo - Mirabello zone. *Nat. Haz. Earth System Sciences*, **12**(11), 3177-3180, doi:10.5194/nhess-12-3177-2012.

Emergeo Working Group (2013): Liquefaction phenomena associated with the Emilia earthquake sequence of May–June 2012 (Northern Italy). *Nat. Haz. Earth Syst. Sci.*, **13**, 935-947.

Galli P., Castenetto S. and Peronace E. (2012): May 2012 Emilia earthquakes (Mw 6, Norterhn Italy): macroseismic effects distribution and seismotectonic implications. *Alpine and Mediterranean Quaternary*, **25**(2), 105-123.

Gruppo di Lavoro Liquefazione (2012): http://ambiente.regione.emilia-romagna.it/geologia/temi/sismica/liquefazione-gruppo-di-lavoro.

Louie J.N. (2001): Faster, better: Shear-wave velocity to 100 meters depth from refraction microtremor arrays. *Bull. Seism. Soc. Am.*, **91**, 347-364

Massa M., Augliera P., Carannante S., Cattaneo M., D'Alema E., Lovati S., Monachesi G., Moretti M. and Piccinini D. (2013): *May-June 2012 Emilia seismic sequence: relocated seismicity*. Project S1, Base-knowledge improvement for assessing the seismogenic potential of Italy, Deliverable D18, Task b2, https://sites.google.com/site/ingvdpcprojects1/home.

Ohori M., Nobata A. and Wakamatsu K. (2002). A Comparison of ESAC and FK Methods of Estimating Phase Velocity Using Arbitrarily Shaped Microtremor Arrays. *Bull. Seism. Soc. Am.*, **92**, 2323-2332.

Okada Y. (1985): Surface deformation due to shear and tensile faults in a half-space. *Bull. Seism. Soc. Am.*, **75**, 1135-1154.

Papathanassiou G., Caputo R. e Rapti-Caputo D. (2012): „Liquefaction-induced ground effects triggered by the 20th May, 2012 Emilia-Romagna (Northern Italy) earthquake". *Annals of Geophys.*, **55**(4), doi: 10.4401/ag-6147.

Pieri M. and Groppi G. (1981): *Subsurface geological structure of the Po Plain, Italy*. Consiglio Nazionale delle Ricerche, Progetto finalizzato Geodinamica, sottoprogetto Modello Strutturale, pubbl. N° 414, Roma, 13 pp.

Pondrelli S., Salimbeni S., Perfetti P. and Danecek P. (2012): Quick regional centroid moment tensor solutions for the Emilia 2012 (northern Italy) seismic sequence. *Annals of Geophys.*, **55**(4), 615-621, doi: 10.4401/ag-6146.

Salvi S., Tolomei C., Merryman Boncori J.P., Pezzo G., Atzori S., Antonioli A., Trasatti E., Giuliani R., Zoffoli S. and Coletta A. (2012): Activation of the SIGRIS monitoring system for ground deformation mapping during the Emilia 2012 seismic sequence, using COSMO-SkyMed InSAR data. *Annals of Geophys.*, **55**(4), 796-802, doi: 10.4401/ag-6181.

Scognamiglio L., Margheriti L., Mele F.M. Tinti E., Bono A., De Gori P., Lauciani V., Lucente F.P., Mandiello A.G., Marcocci C., Mazza S., Pintore S. and Quintiliani M. (2012): The 2012 Pianura Padana Emiliana seismic sequence: locations, moment tensors and magnitudes. *Annals of Geophys.*, **55**(4), 549-556, doi: 10.4401/ag-6159.

Stephenson W. J. , Louie J. N., Pullammanappallil S., Williams R.A., Odum J.K., Okada Y. (2005): Blind Shear-Wave Velocity Comparison of ReMi and MASW Results with Boreholes to 200 m in Santa Clara Valley: Implications for Earthquake Ground-Motion Assessment. *Bull. Seism. Soc. Am.*, **95**(6), 2506-2516.